GROUND NOISE STUDIES USING THE TAMA300 GRAVITATIONAL-WAVE DETECTOR AND RELATED HIGHLY-SENSITIVE INSTRUMENTS

Akito ARAYA
Earthquake Research Institute, University of Tokyo,
1-1-1, Yayoi, Bunkyo, Tokyo 113-0032, Japan

1. INTRODUCTION

Detection of gravitational waves will open up significant fields of study in physics and astronomy: investigation of the nature of the waves and, more importantly, observation of astronomical phenomena through a new channel. Examples are estimation of the angular momentrum just before a supoernova explosion, and a gravitational waveform from coalescing binary neutron stars. The latter defines parameters of the binary system, and therefore the distance to the source can be estimated from an amplitude of the waveform; this leads to the strict determination of the Hubble constant [1] as well as to the verification of the general relativity in the strong field. Although emission of gravitational waves from a neutron-star binary system was confirmed [2], no one has ever succeeded in the direct detection of gravitational waves.

In order to detect gravitational waves and establish a field of gravitational-wave astronomy, several gravitational-wave detectors are under construction (Table 1): LIGO [3] in the U.S., VIRGO [4] and GEO [5] in Europe, and TAMA [6] in Japan. These laser-interferometric detectors have large baseline lengths, from 300m to 4km. It is because the gravitational-wave signals, expressed by a strain of spacetime, are expected to be very small (Table 2) and the gravitational wave detectors inevitably have long baseline to enhance signal amplitudes. This means that the gravitational wave detectors are subject to earth strain variations due to their long baselines.

Table 1 Projects of Interferometric Gravitational-wave Detectors

Project	Countries	Baseline, Site	Observation (scheduled)
LIGO	U. S. A.	4km, Hanford 4km, Livingston	2002
VIRGO	France / Italy	3km, Pisa (Italy)	2005
GEO	Germany / U. K.	600m, Hannover (Germany)	2002
TAMA	Japan	300m, Mitaka (Tokyo)	2000

Table 2 Gravitational-wave sources

Source	Frequency (Hz)	Distance (pc)	Expected Strain	Event Rate
Binary Neutron Stars	10 ~ 1k	200M	$4*10^{-22}$	several /year
Supernova	~ 1k	15M	$1*10^{-21}$	several /year
Pulsar	~ 1k	10k	$1*10^{-25}$	continuous

Although gravitational-wave signals, which are in the frequency range of ~10Hz to ~1kHz, can be distinguished from the earth strain signals (< 1Hz), long-term stability of the detector is affected by the earth strain variation at low frequencies. For this reason, gravitational wave detectors usually have feedback circuits to compensate such disturbances. The feedback signal contains the low-frequency disturbances, and these low-frequency noises are considered to be "signals" from a geophysical viewpoint. In fact, we have successfully observed geophysical signals using the TAMA300 and a 20-m gravitational-wave detector constructed underground. In this paper, after overview of the TAMA300 detector and its current results, demonstrative geophysical observations using the TAMA300 and the underground detector are described. Possible geophysical sources are also discussed.

2. TAMA300 DETECTOR

TAMA300 is a gravitational-wave detector with a 300-m-long L-shaped interferometer constructed in National Astronomical Observatory (Mitaka, Tokyo). The project started in 1995, and several observation runs were carried out from 2000 [7, 8]. Optical and control design of the TAMA300 detector is shown in Fig. 1; light from a 10-W laser passes through a 10-m ring-type mode cleaner to adjust beam geometry, and output light illuminates a main interferometer which has two 300-m Fabry-Perot optical cavities located orthogonally to each other. Very small mirror motions excited by gravitational waves are enhanced by the optical cavities, and are detected as fringe variations in the interferometer. To keep the cavities on resonance, feedback circuits are used for controlling mirror position and laser frequencies.

As shown in Fig. 2, several noise sources define the detector sensitivity, and ground motion is the major noise source at low frequencies. Since test masses, i.e. mirrors, are suspended to work as inertial references, seismic noise near the resonant frequency excites large mirror motion and degrades the detector sensitivity. Disturbances at low frequencies, such as tectonic earth strain change, barometric response of the ground, pumping of ground water, earth tides, are compensated by the feedback circuits to some degree. In fact, however, other practical disturbances often make the circuits go beyond the control range in the long-term operation resulting in loss of duty cycle.

Figure 3 shows an operation status in a 1200-hour data-taking run carried out from August 1 to September 20 in 2001. The resulted duty cycle is 92.25%. The main reasons for losing operation are thermal drift of the vibration isolation system, and excitations by constructions and typhoons. At underground, thermal variation and these excitations are very small. It is ideal to construct gravitational wave detectors underground from the point of long-term stable

observation. Details of a 20-m gravitational wave detector constructed underground in a mine is described later in Section 4.

Currently the TAMA300 is capable of detecting two-1.4solarmass-neutron-star binary coalescence in our galaxy. The TAMA project has ended in March 2002, and the research is continuing under post-TAMA program; sensitivity of the TAMA300 detector is improving (Fig. 4).

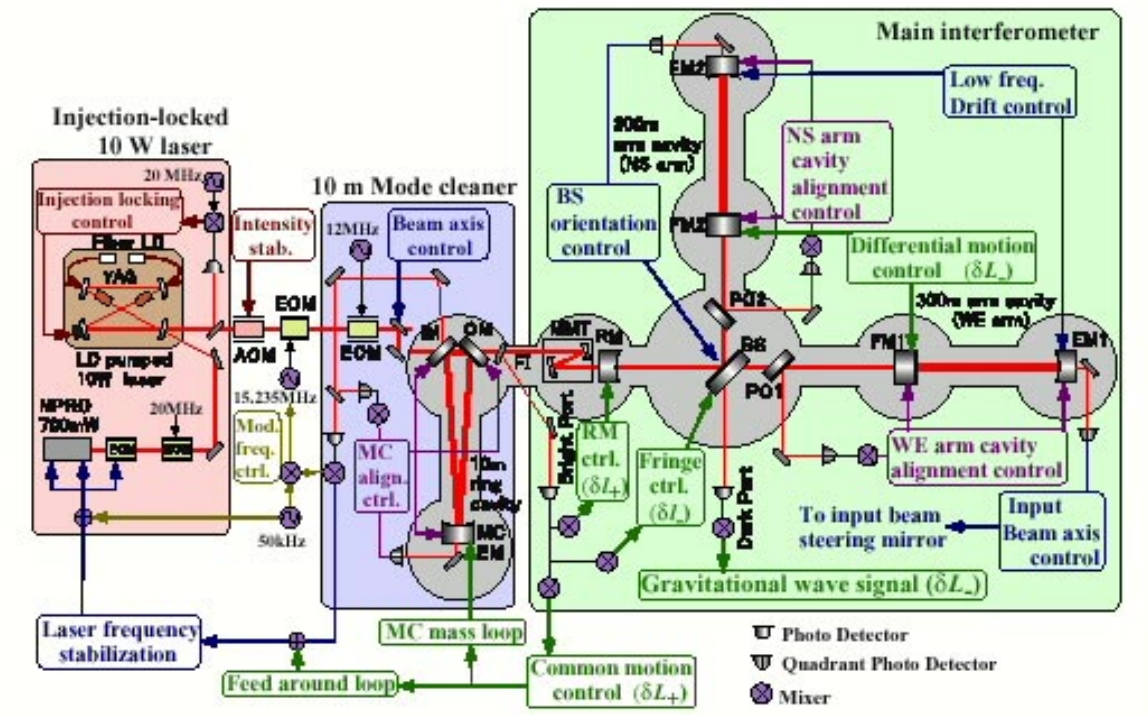

Fig. 1 Optical and control design of the TAMA300 detector.

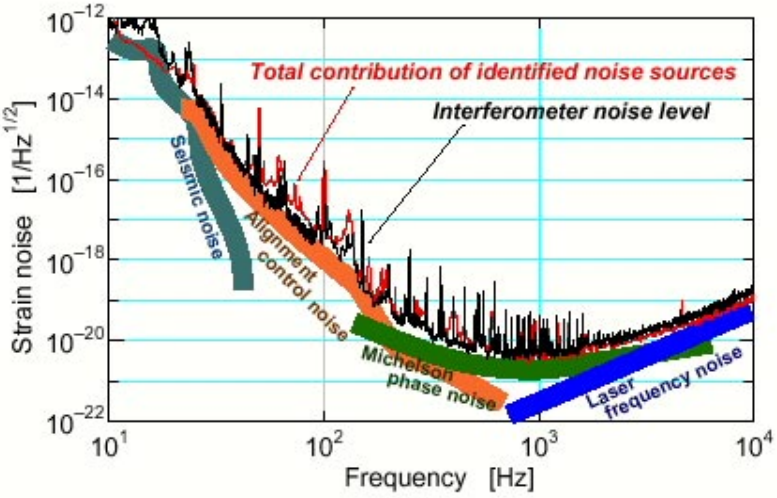

Fig. 2 Noise sources of the TAMA300 detector.

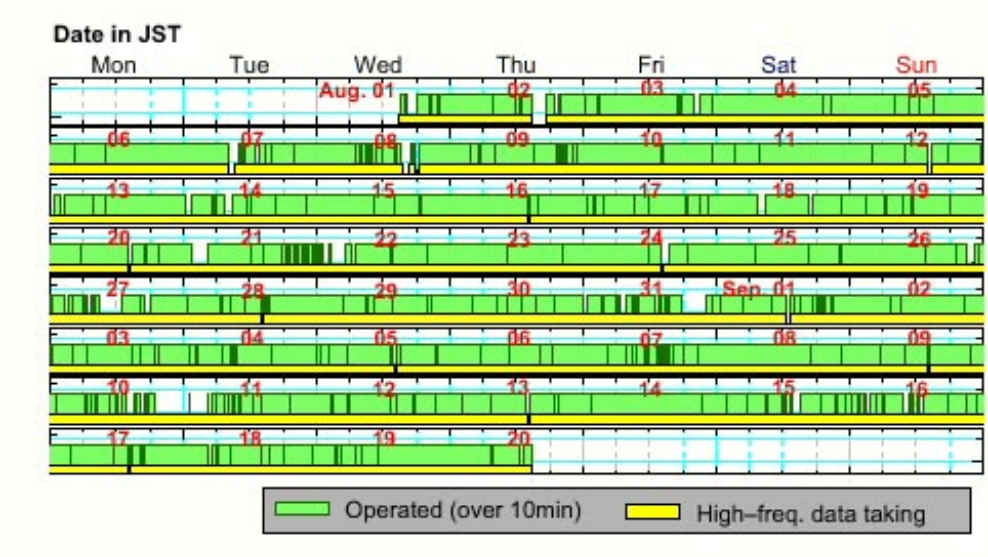

Fig. 3 Operation status in a 1200-hour data-taking run (Aug.1 ~ Sep.20, 2001).

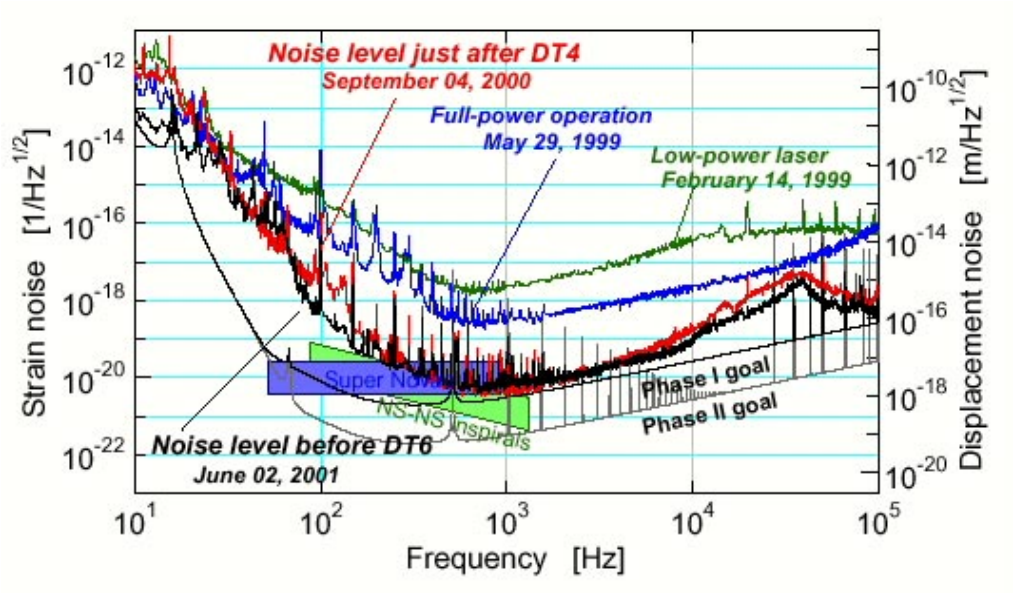

Fig. 4 History of sensitivity and expected gravitational-wave signal levels.

3. ABSOLUTE-LENGTH OBSERVATION USING A TAMA CAVITY

We have developed a novel method by which the cavity length can be determined with excellent accuracy [9]. This method has been applied to absolute-length measurements of one arm of the TAMA300 optical cavities with a 300-m baseline. Long-term variations in the cavity

length were successfully observed with an accuracy of ~1μm. Variations in the cavity length included an earth-strain change due to groundwater pumping, atmospheric pressure change, and earth tides [10].

3.1 Measurement system

The principle of the method is shown in Fig. 5. Assuming that phase-modulated light with a small modulation index illuminates the Fabry-Perot cavity, two sidebands are included at both sides of the carrier. If the carrier frequency is tuned at the center of a resonance, and at the same time the sideband frequencies are tuned at the center of other resonances, the following relation is satisfied:

$$\nu_m = n\, c/(2L), \tag{1}$$

where c is the speed of light and L is the cavity length. If the order n (integer) is known, the absolute length of the cavity can be derived from the modulation frequency. A high-finesse cavity allows precise locking to the center of the resonance, resulting in an accurate measurement of the absolute length. Therefore, the accuracy of L is expected to be improved by a factor of the finesse (F), as compared with conventional round-trip methods.

The measurement accuracy (δL) depends on the phase resolution ($\delta\phi$) of the measurement,

$$\delta L = (c/2\nu_m)\,(\pi/F)\,(\delta\phi/2\pi). \tag{2}$$

In a practical system $\delta\phi/2\pi$ tends to be at best $10^{-4} \sim 10^{-5}$ in the conventional round-trip (π/F=1) distance measurement system [11]. In this method, by virtue of an improvement of the phase resolution by a factor of π/F, owing to the sharp resonance of the cavity, the accuracy of a measurement is expected to be $\delta L \sim 8*10^{-7}$m, assuming $\delta\phi/2\pi=10^{-5}$, ν_m=12MHz, and the TAMA parameters (L~300m, F=520).

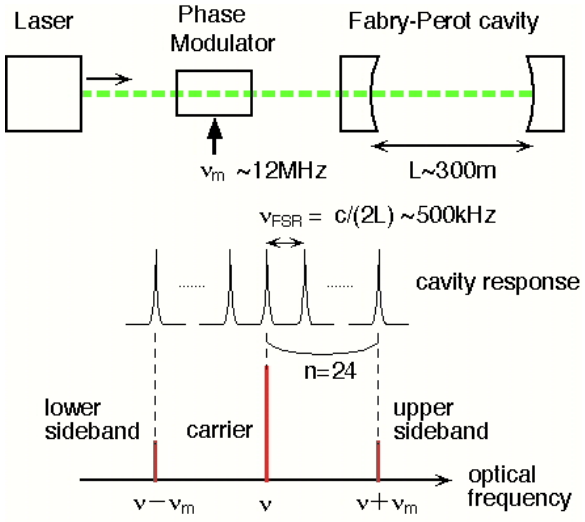

Fig. 5 Principle of the absolute-length measurement.

As shown above, this method requires three steps: carrier locking, sideband locking, and counting the modulation frequency. A block diagram of the measurement system is shown in Fig. 6. The laser carrier frequency is locked to the cavity using the Pound-Drever method. The modulation frequency from a voltage-controlled crystal oscillator (VCXO) is locked so that the resulting sidebands are resonating in the cavity. To maintain the measurement accuracy, the frequency counter is locked to a stable (uncertainty < 10^{-11}) GPS timebase.

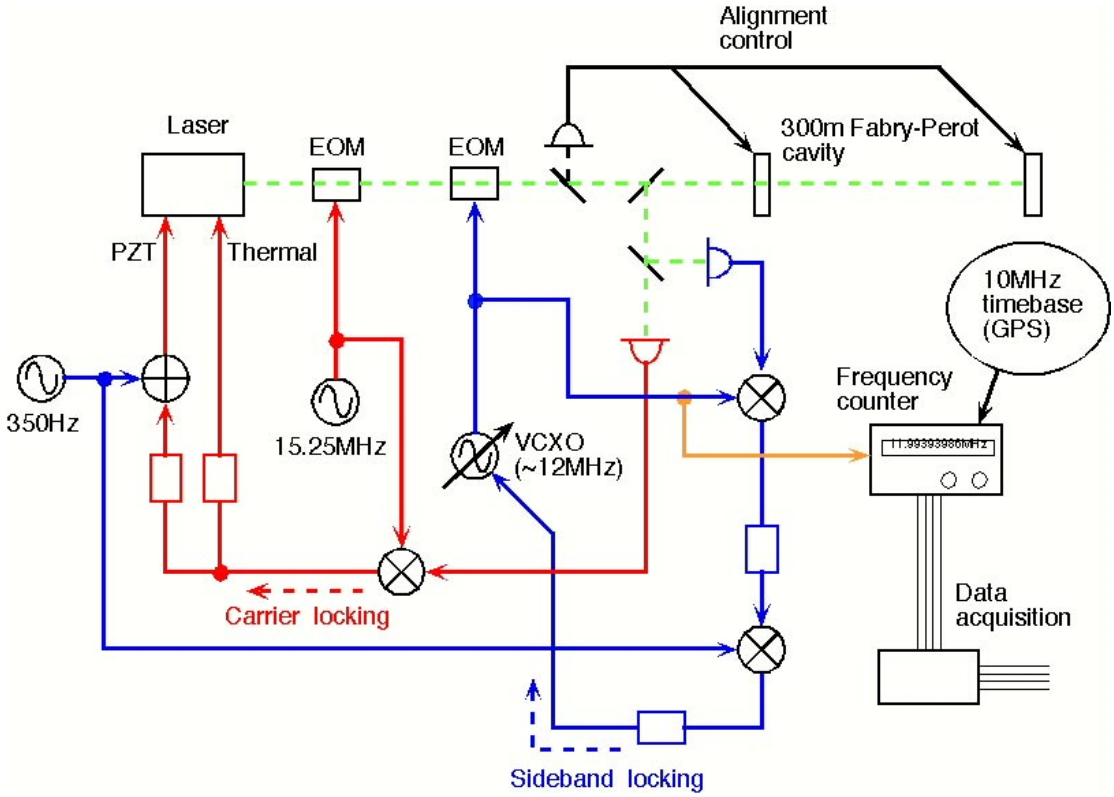

Fig. 6 Block diagram of the measurement system.

3.2 Observation and Data analysis

The observation was carried out during 13 to 23 March 1998, and a part of the data (22:00JST 18 March to 12:00JST 23 March) was found to be valid. Figures 7(a)~(c) resulted from the measurement.

Figure 7(a) shows the modulation-frequency change (left axis) and the corresponding absolute length of the cavity with the offset length subtracted (right axis). Two striking features can be seen: one is many spikes appearing during the daytime; the other is a long-term drift over a period of several days. A magnified view (Fig. 7(b)) shows that these spikes have a rapid rise within about 30 minutes, and relaxation within a few hours. The amplitude is about 20μm. In our research, these spikes were synchronized with the pumping of groundwater, as shown in Fig. 7(c), indicating a correspondence between the rise of a spike and the groundwater pumping. The location of the groundwater pump was about 200m from the center of the cavity.

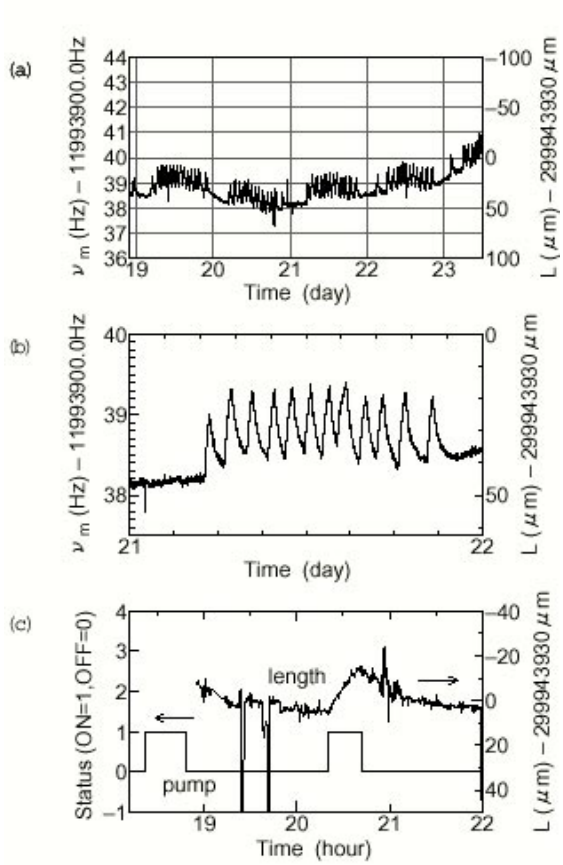

Fig. 7 Absolute length of the 300-m TAMA cavity during 18 to 23 March 1998.

To extract a long-term component from the data, we tried to remove these artificial spikes. It was assumed that the ground strain is proportional to the volume of groundwater in a reservoir ($v(t)$), which is connected with other neighboring reservoirs (Fig. 8).

In this model, the volume of groundwater satisfied

$$dv/dt = - p + q_0 (v_0 - v), \qquad (3)$$

where the assumed parameters of this model are the start (t_0) and stop (t_1) time of pumping, the pumping speed ($p(t)$=const. for $t_0 \leq t \leq t_1$, otherwise $p(t)$=0), the permeability of the water supply from neighboring reservoirs (q_0), and the initial volume of the reservoir (v_0). These parameters were fitted to the data, and the spikes were removed.

The result after removing the spikes is shown in Fig. 9 as "residual". The long-term component shows a barometric response, thermal drift, and tidal effects. As for the tidal effects, a spectrum analysis shows a semi-diurnal component whose amplitude is similar to the theoretical one with the standard tidal parameters. On the other hand, the observed barometric response was considered to be the ground strain change caused by a change in the atmospheric

load on the ground. Some geophysical observations also show a similar amount of ground-strain response to the atmospheric pressure ((1~10)*10^{-9}/hPa) [12].

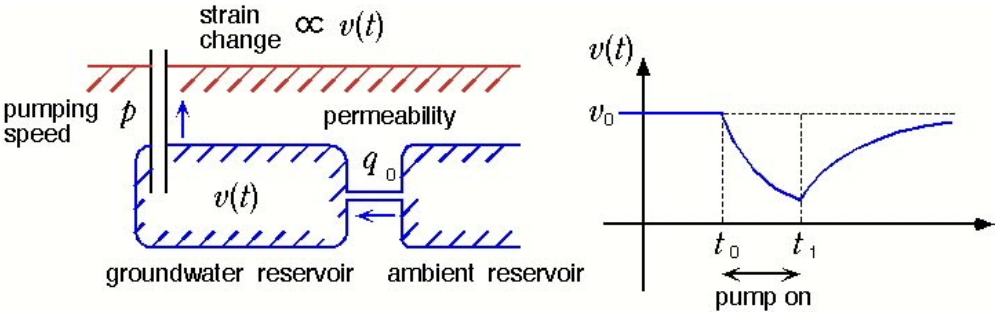

Fig. 8 Model of ground strain due to groundwater pumping.

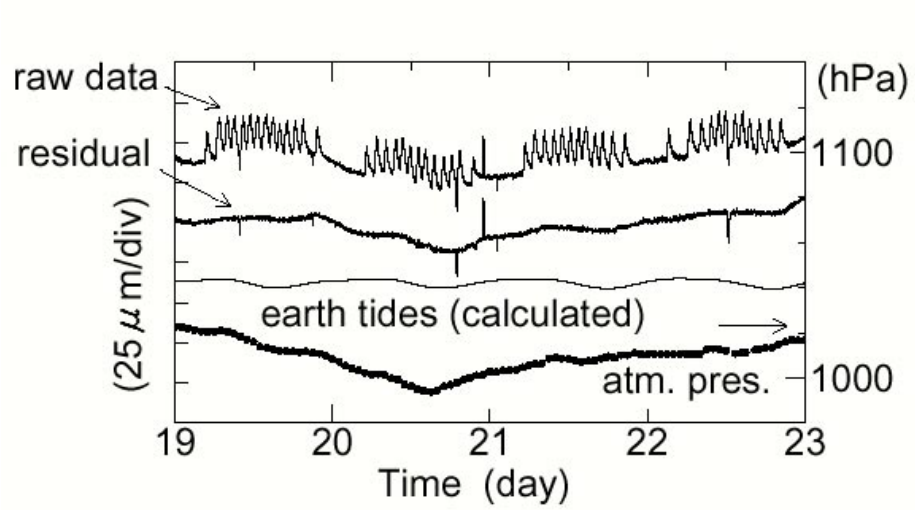

Fig. 9 Change in the cavity length after removing effects of groundwater pumping.

4. EARTH TIDES OBSERVED BY AN UNDERGROUND DETECTOR

The earth strain data observed by the TAMA300 shows several noise sources such as pumping of groundwater, atmospheric pressure, and temperature drift. In the underground site, these sources may have less effect on the detector. Stability of underground environment is considered to be good for long-term stable observation of gravitational waves as well as of earth strain. For this reason, a gravitational wave detector with 20-m-long interferometers was constructed (Fig. 10) at 1000-m underground in the Kamioka Mine which is famous for the site of the Super-Kamiokande neutrino detector [13]. Ground noise level compared with the TAMA site is shown in Fig. 11; below ~100Hz, the noise level is one to two orders of magnitude lower in the Kamioka site. Kamioka Mine is also a planned site of the future gravitational-wave project, LCGT [14], and we started feasibility studies using the 20-m detector and a 100-m

detector which is now under construction and will have cryogenic mirrors to reduce thermal noise.

Fig. 10 A 20-m-long detector constructed at 1000-m underground in Kamioka Mine.

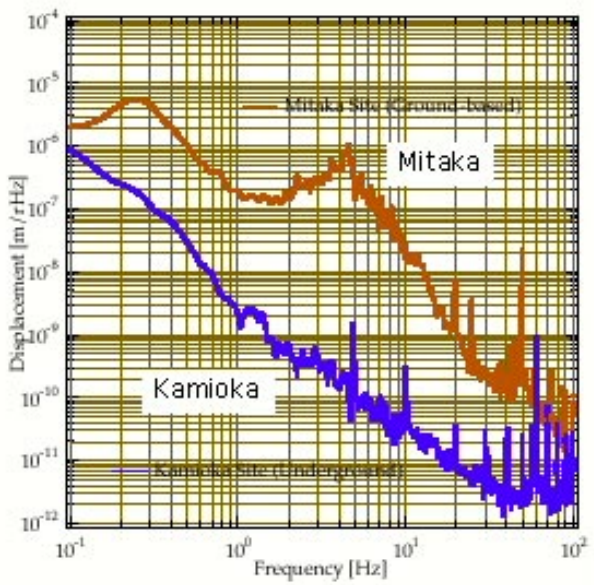

Fig. 11 Ground noise level at Kamioka site compared with the TAMA (Mitaka) site.

We have obtained long and high-quality data from the 20-m detector since a quiet ground motion helped to keep an operation very stable; with well-aligned condition, duty cycle reached as much as 99.8%. Figure 12 ("Observed") shows a laser feedback signal which is used to keep the cavity on resonance and changes according to the earth strain variation and drift of the laser

frequency. Apparently, earth tides, which are dominated by diurnal and semi-diurnal signals, can be seen in the observed data; it should be noted that, as compared with the data in Fig. 9, tidal signals in Kamioka are very clear even with a short-baseline detector, showing very low background in Kamioka underground site. Using tidal analysis program, BAYTAP-G [15], based on Bayesian information criterion, we can extract tidal components from the raw data. The residual, which is considered to be mainly drift of the laser frequency, is shown as "Trend" in Fig. 12.

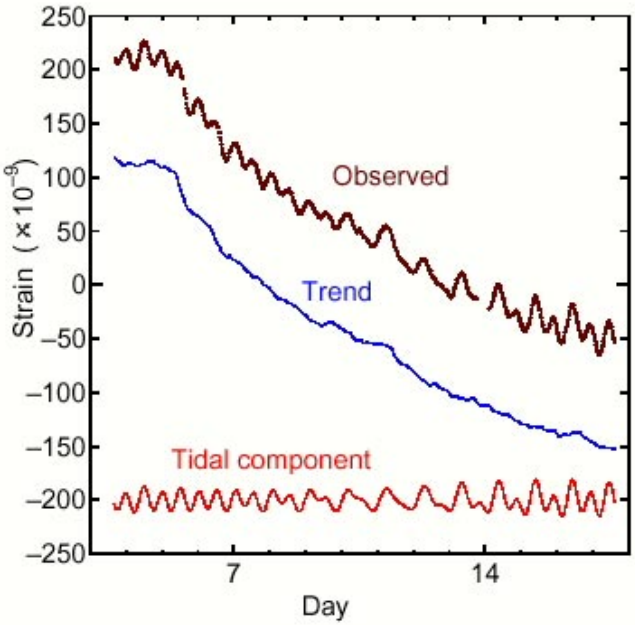

Fig. 12 Laser feedback signal used to lock the 20-m cavity on resonance. It changes according to the earth strain variation and drift of the laser frequency.

5. CONCLUSIONS

In this paper, the current status of TAMA300 detector and demonstrative geophysical observations using gravitational wave detectors are described.

We successfully observed a long-term change in the 300-m cavity in terms of the absolute length using the TAMA detector. The accuracy of the measurement was about 1μm, which corresponds to $3*10^{-9}$ in strain. The cavity length was affected mainly by artificial ground strain change due to groundwater pumping. After removing these artificial spikes with a simple groundwater model, we could obtain long-term variations which seemed to be the ground-strain response of the barometric pressure, thermal drift, and earth tides. Because this measuring method is based on the detection of absolute value, it has great advantage for a long-term or a secular strain monitor, which includes tectonic strain accumulation (10^{-7}~10^{-8}/year in Japan),

near-fault strain variation, long-period earth's free oscillations, and a distance determination in metrology.

In Kamioka Mine observation using the 20-m detector, we have shown a stable data acquisition and high quality data including earth tides. If the planned LCGT detector with 3-km-long interferometers is constructed in the Kamioka Mine, it would be very useful tool for geophysics as well as gravitational-wave astronomy. Possible geophysical sources are summarized in Table 3. Superconducting gravimeters, which have a resolution of 10^{-10}~10^{-11} m/s^2, can detect some of these sources. With a km-baseline underground detector, we expect to find out some sources that have never been detected even with the superconducting gravimeters.

Table 3 Possible geophysical sources

Source	Period	Amplitude (m/s^2)	Expected Strain
Earth's free Osc. (seismic)	10^2~10^3s	10^{-6}~10^{-8}	10^{-8}~10^{-10}
Earth's free Osc. (background)	10^2~10^3s	~10^{-11}	~10^{-13}
Core modes	~10^3s	~10^{-11}	~10^{-13}
Core undertone	10^3~10^4s	~10^{-11}	~10^{-13}
Earth tides	10^4~10^5s	~10^{-6}	~10^{-8}
Co-/post-seismic movements	1~10^2day	10^{-6}~10^{-8}	10^{-5}~10^{-6}
Crustal movements	10^2day~	10^{-7}~10^{-9}	10^{-7}~10^{-9}

6. REFERENCES

[1] B. F. Schutz, Nature 323, 310 (1986).

[2] J. H. Taylor and J. M. Weisberg, Astrophys. J. 345, 434 (1989).

[3] A. Abramovici et al., Science 256, 325 (1992).

[4] The VIRGO Collaboration, *VIRGO Final Design Report*, VIR-TRE-1000-13, 1997.

[5] K. Dantzmann et al., Max-Planck-Institut fuer Quantenoptik Report No. 190, 1994.

[6] K. Tsubono, in *Gravitational Wave Experiments*, edited by E. Coccia, G. Pizzella, and F. Ronga (World Scientific, Singapore, 1995), pp. 112-114.

[7] H. Tagoshi, N. Kanda, T. Tanaka, D. Tatsumi, S. Telada, and the TAMA collaboration, Phys. Rev. D 63, 1 (2001).

[8] M. Ando et al., Phys. Rev. Lett. 86, 3950 (2001).

[9] A. Araya et al., Appl. Opt. 38, 2848 (1999).

[10] A. Araya, in *Gravitational Wave Detection II*, edited by S. Kawamura, and N. Mio (Universal Academy Press, Inc., 2000), pp. 165-170.

[11] K. M. Baird, Metrologia 4, 135 (1968).

[12] H. Hikawa et al., Quarterly Journal of Seismology (Japan Meteorological Agency, Tokyo) 47, 91 (1983) (in Japanese).

[13] K. Hirata et al., Phys. Rev. Lett. 58, 1490 (1987).

[14] K. Kuroda et al., Int. J. Mod. Phys. D 8, 557 (1999).

[15] Y. Tamura, T. Sato, M. Ooe, and M. Ishiguro, Geophys. J. Int. 104, 507 (1991).